

Simulation Of Mono And Dual-Wavelength Airborne Radar Observations Of Precipitating Systems At Various Frequency Bands

VALENTIN LOUF¹, OLIVIER PUJOL¹, HENRI SAUVAGEOT², JÉRÔME RIEDI¹, AND GUILLAUME PÉNIDE¹
¹Université Lille 1, LOA Laboratoire d'Optique Atmosphérique ²Université Toulouse III, Observatoire Midi-Pyrénées



1. Introduction

Meteorological hazard in civil aviation is mainly due to convective precipitating systems, and particularly hail and strong turbulence areas. A radar located behind the radome, forming the noise of the plane, is the only tool used to detect these precipitations. The question of the most efficient couple (f , θ_{3dB}) has to be set for airborne radar precipitating system observations, where f is the microwave frequency and θ_{3dB} the beamwidth aperture at 3 dB ($\theta_{3dB} = 70\lambda/D$, D is antenna diameter). We also studied the interest of the dual-wavelength technic.

2. Method

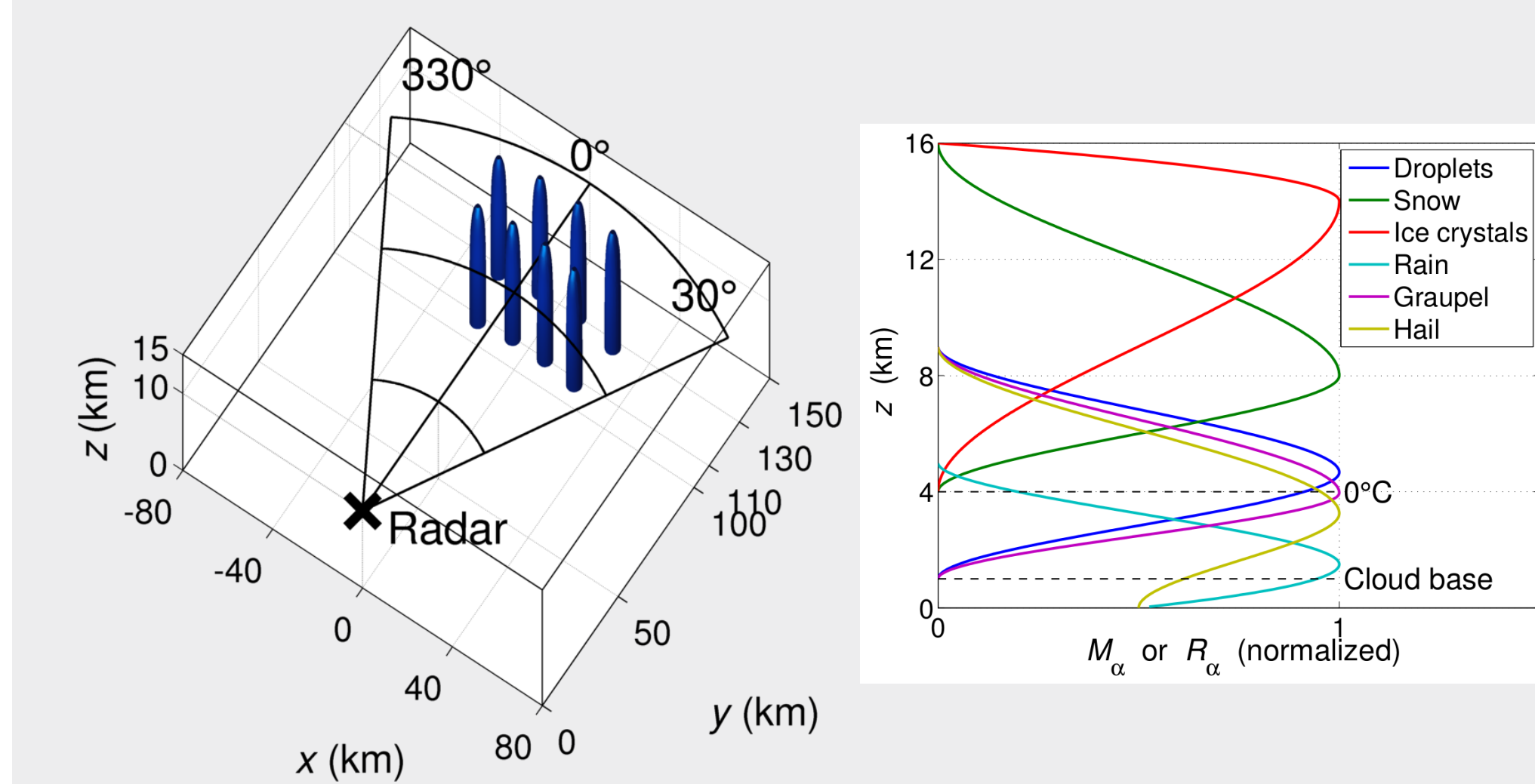


Figure 1: (a) System configuration. Convective towers are surrounded by a stratiform background (b) Hydrometeor normalized vertical distribution.

A realistic model of precipitating systems is used to perform simulations of airborne radar observations at the six meteorological frequency bands: S ($f \approx 3$ GHz), C (5.5 GHz), X (10 GHz), K_u (15 GHz), K_a (35 GHz), and W (94 GHz). The airborne radar is located at 10 km of altitude. Range bin spacing is set to 150 m. The electromagnetic energy is supposed to be uniformly distributed.

References

- [1] Valentin Louf et al. Simulation of airborne radar observations of precipitating systems at various frequency bands. *IEEE TGRS*, 2013.
- [2] Valentin Louf et al. The dual-wavelength method for hailstorm detection by airborne radar. submitted to *IEEE TGRS*.

3. Frequency and θ_{3dB} comparison

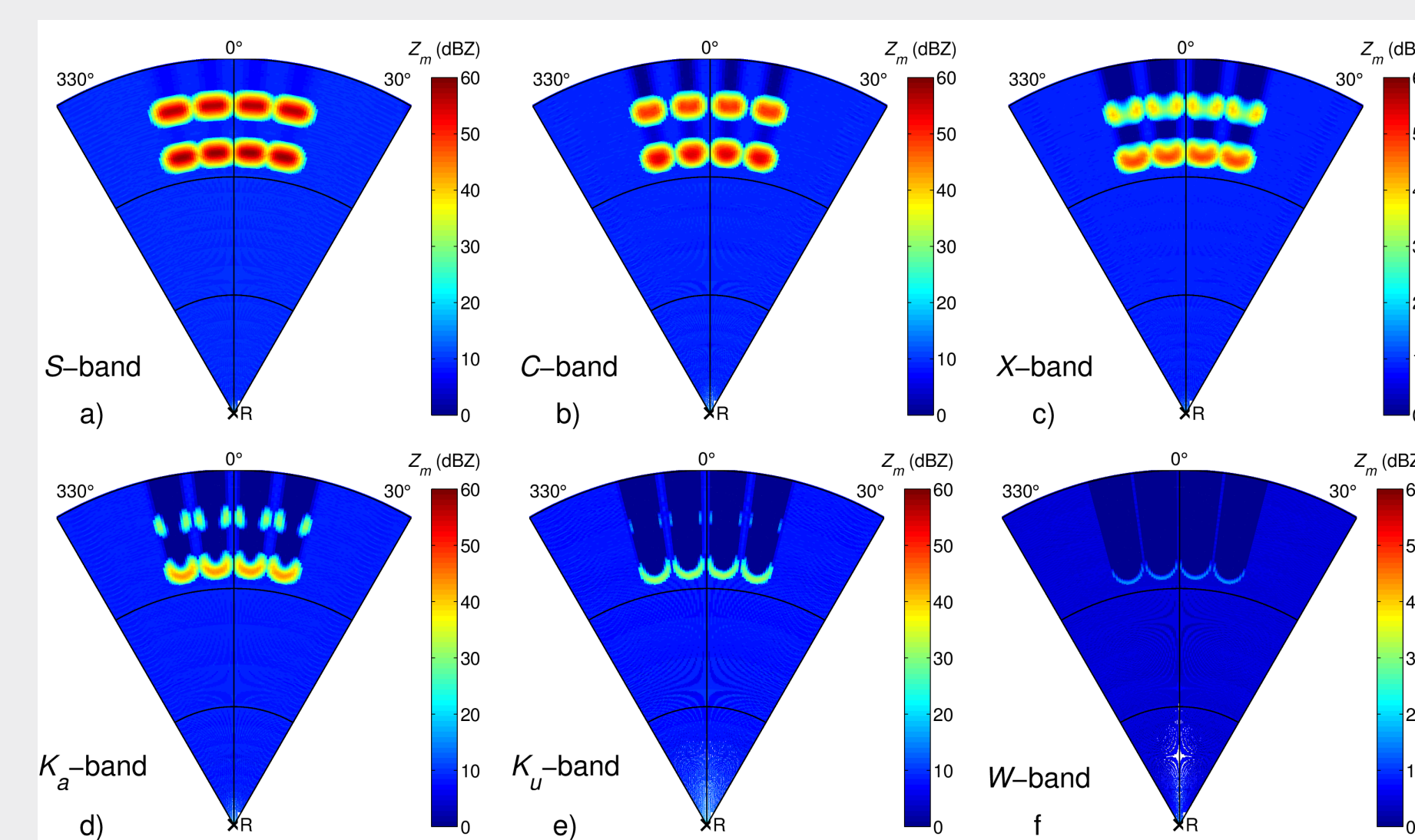


Figure 2: The frequency effect. (a,b) Antenna diameter $D_a = 2$ m, and (c,d,e,f) $D_a = 0.8$ m. All convective towers contain hail (here $R_h = 40$ mm h^{-1})

S and C -bands, two lines of convection are clearly visible. X -band the second row is attenuated and seems to be safe. K_u , K_a , and W -bands, the convective system is unobservable.

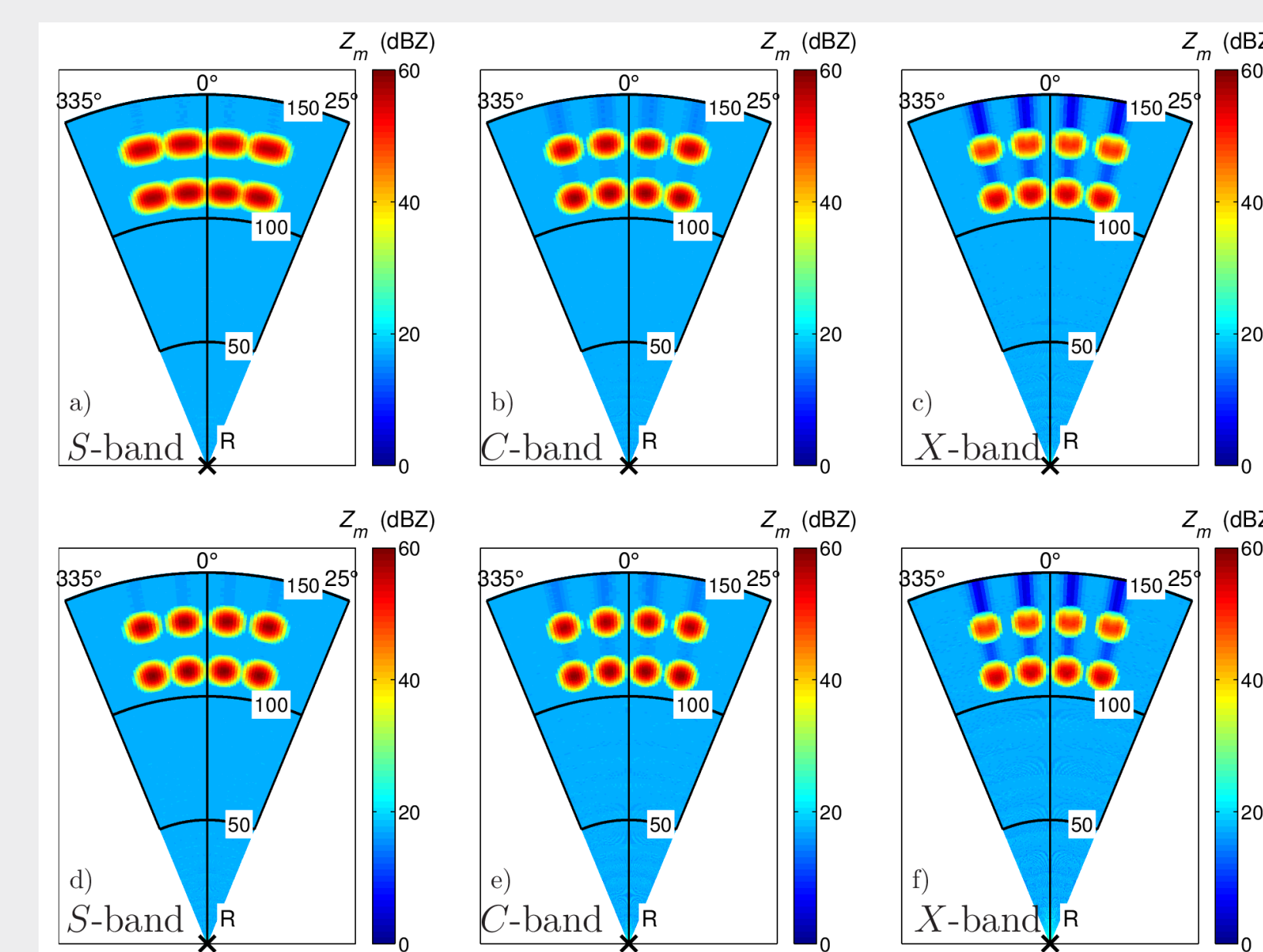


Figure 3: The θ_{3dB} effect. PPI view simulation of the measured reflectivity Z_m in a mesoscale system at various frequency bands: S (a,d), C (b,e), X (c,f), with a radar antenna size of 2 m (a,b,c) and of 4 m (d,e,f).

X -band presents a good improvement for $D = 2$ m, since the convective towers are separated. For $D = 4$ m, convective towers are identifiable.

Conclusion and further studies

We have studied the effect of different parameters: f , θ_{3dB} , rainfall and hailfall rate, and DW configuration. For this, more than 400 systems (purely numerical or inspired from reality) have been computed. Due to the relation $\theta_{3dB} \propto \lambda/D$, decreasing θ_{3dB} implies decreasing λ and increasing D . The simulation presented herein on modelled precipitating systems shows that (1) S -band

4. Dual-wavelength technic (DWT)

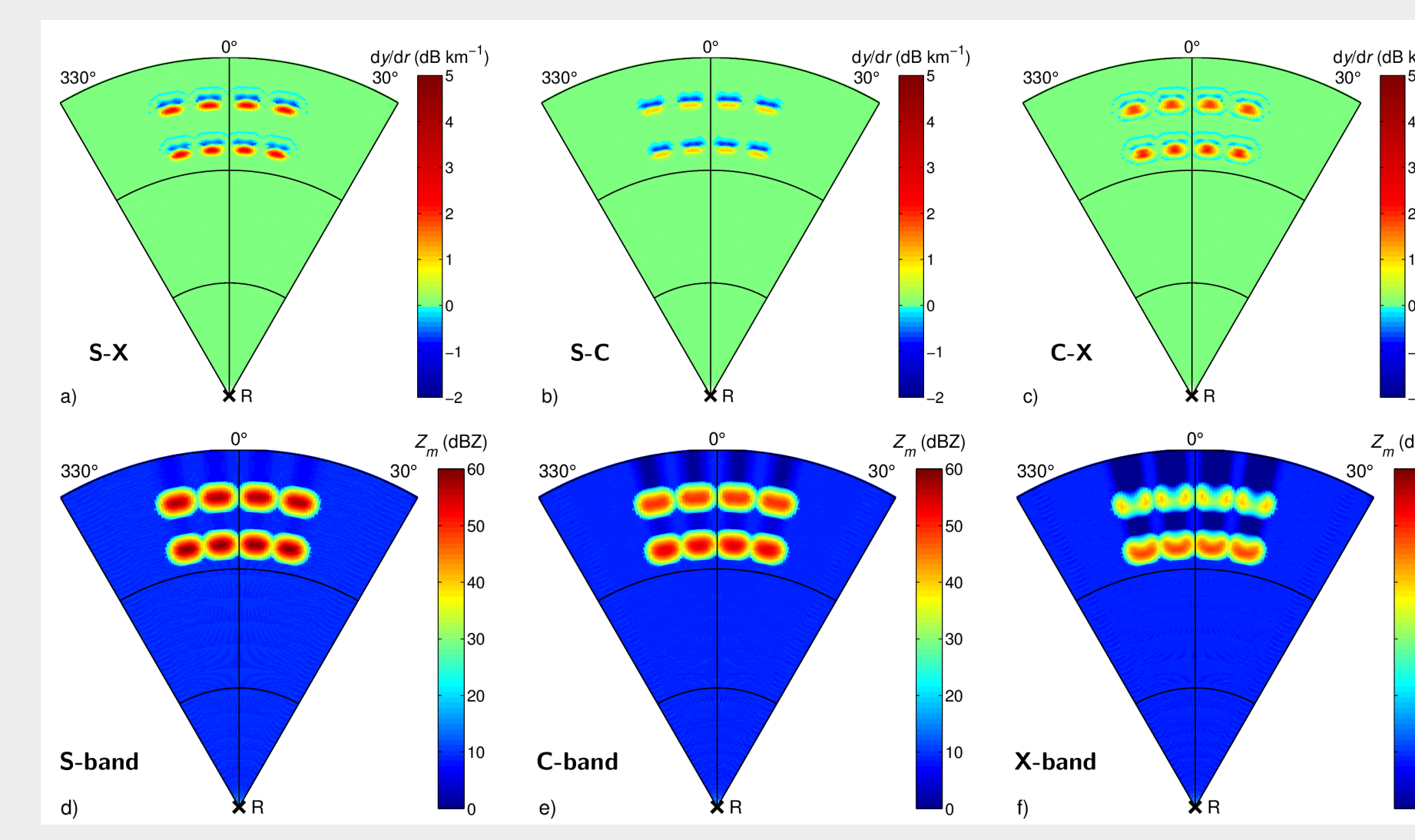


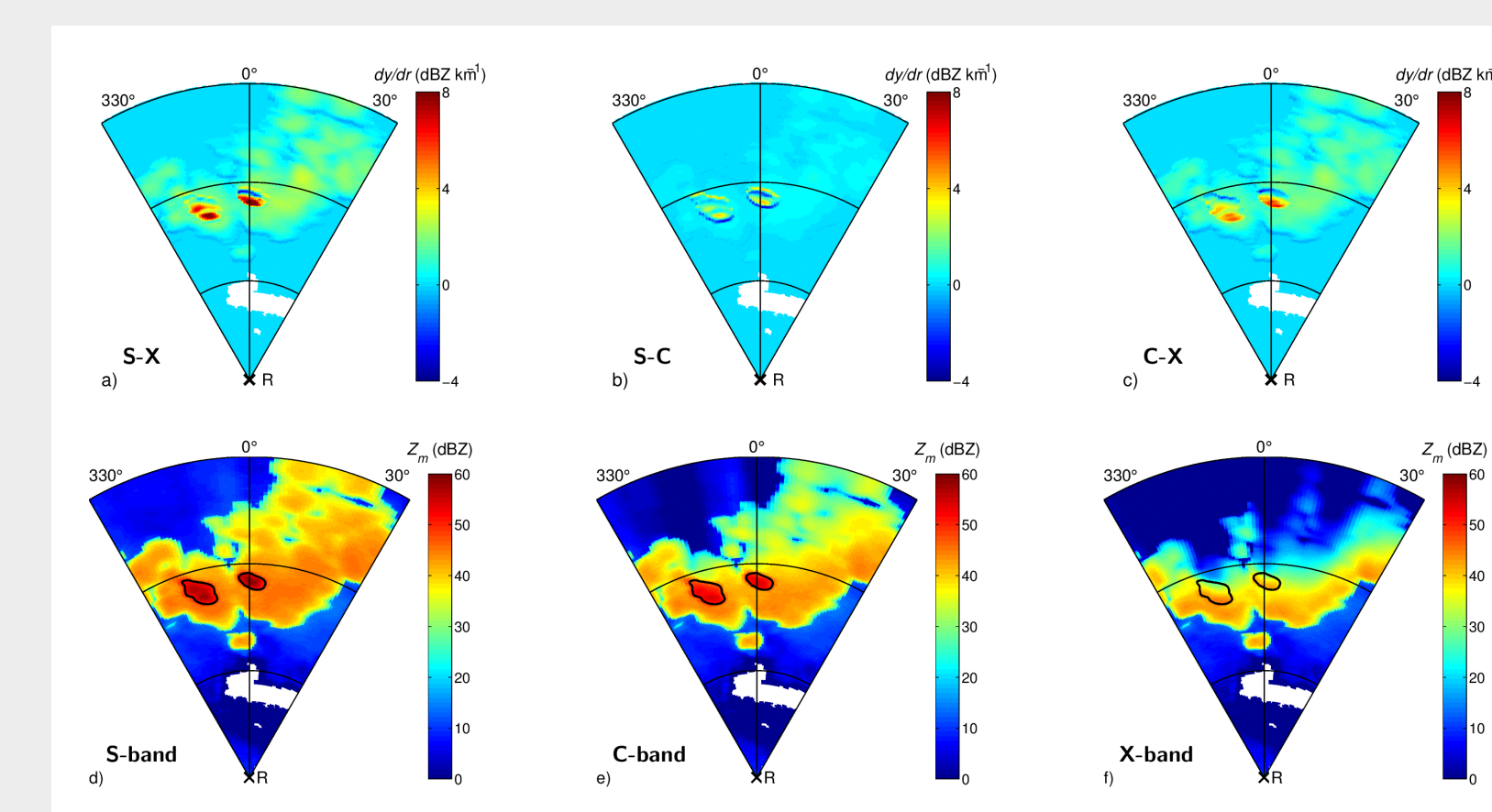
Figure 4: Gradient of the dual-wavelength reflectivity difference relative to the distance for (a) S - X , (b) S - C , and (c) C - X . Reflectivity field for (d) S , (e) C , and (f) X -bands for $\theta_{3dB} = 3^\circ$.

The quantity studied is the dual-wavelength ratio (DWR) dy/dr :

$$\frac{dy}{dr} = \frac{d}{dr} [Z_{m,\lambda_1}(r) - Z_{m,\lambda_2}(r)]. \quad (1)$$

where Z_m is the measured reflectivity at a wave-

5. Real mesoscale system



In order to illustrate the usefulness of the DWR to determine hail areas, let consider a real mesoscale precipitating system that occurs on May 2003, 2nd in Alabama (USA). Note that the area C does

length l or s (for large or small). It requires that the two radar beams illuminate identical volumes of resolution, the same value of $\theta_{3dB} = 3^\circ$ has been considered at S , C , and X -bands. The use of the DWR is interesting because hail is the only non-Rayleigh scatterer at these frequency bands, and thus it implies that DWR is positive in front of a hail tower and always negative at the rear, and this can be used as .

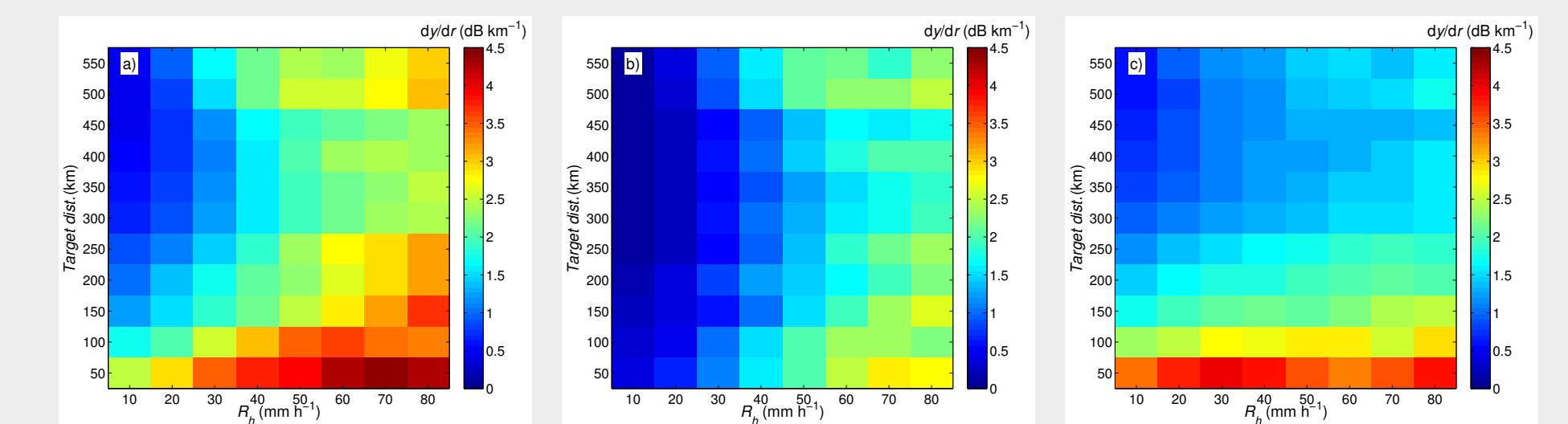


Figure 5: Gradient of the dual-wavelength reflectivity difference relative to the distance for (a) S - X , (b) S - C , and (c) C - X . Reflectivity field for (d) S , (e) C , and (f) X -bands for $\theta_{3dB} = 3^\circ$.

dy/dr increases with R_h , small variations are due to Mie modes.

Figure 6: PPI field of dy/dr of hailstorm for S - X (a), S - C (b), and C - X (c). Measured reflectivity in dBZ at S (d), C (e), and X -bands (f). CAPPI at 10 km of altitude of the mesoscale system of May 2003, 2nd, in Alabama (USA). R indicates airborne radar position. Data comes from NEXRAD network (S -band). Radar designation is KFCC. Black contours delimitate possible hail area ($Z_m > 45$ dBZ). White zone between 30 and 50 km corresponds to an absence of data.

not contain hail, although it presents a reflectivity which is about that of areas A and B . It illustrates that a criteria based solely on reflectivity is not sufficient for hail detection.

Contact Information

Web www-loa.univ-lille1.fr
Email valentin.louf@ed.univ-lille1.fr
Phone +33 (0)3 20 43 43 11
 Scan this QR code to download this poster and more informations about this work.

